

# Agriculture: Rice Cultivation Emissions Model Methodology



## 1. Preview Statement

Rice paddy fields play an important role in greenhouse gas emissions as a source of methane ( $\text{CH}_4$ ) emissions. Current estimates of  $\text{CH}_4$  emissions from rice cultivation are mostly derived from agricultural statistics (Carlson et al., 2017; Fung et al., 1991; Li et al., 2002; Saunio et al., 2016; Saunio et al., 2020; Yan et al., 2009; Zhang et al., 2016). These reports are usually aggregated to country level, and have high levels of uncertainty. Rice cultivation varies between regions and inaccurate estimates of rice cropping intensities reported in the agricultural statistics can lead to high uncertainty in the estimate of  $\text{CH}_4$  emissions (Zhang et al., 2020).

Satellite-based annual rice cultivation map is a spatially resolved method that can improve the estimation of  $\text{CH}_4$  emission from rice paddies. It is supported by results of a recent study by (Zhang et al., 2020) that showed rice cultivation area and cropping intensities derived from Moderate Resolution Imaging Spectroradiometer (MODIS) satellite imagery for monsoon Asian countries (the south, east and southeast Asian countries). This study presents strong spatial temporal consistencies with atmospheric methane concentration datasets derived from greenhouse gas monitoring satellites: the Scanning Imaging Absorption Spectrometer for Atmospheric Chartography (SCIAMACHY) on the Environmental Satellite (ENVISAT) and the Thermal and Near Infrared Sensor for Carbon Observation Fourier-Transform Spectrometer (TANSO-FTS) onboard the Greenhouse Gases Observing Satellite (GOSAT). Thus, here, we employ the Paddy Watch method that uses satellite-data from MODIS measurements to identify global rice fields and apply a  $\text{CH}_4$  emissions equation to estimate rice fields emissions.

## 2. Model Deployment

Global  $\text{CH}_4$  emissions from rice cultivation strongly depend on global harvested rice extent. A simple approach was used to estimate  $\text{CH}_4$  emissions from rice cultivation which is given by equation 1:

$$\text{Emission} = A \times EF \text{ (Eq.1)}$$

Where *Emission* is the  $\text{CH}_4$  emissions ( $\text{g CH}_4 \text{ year}^{-1}$ ), *A* is the rice paddy annual harvested area ( $\text{m}^2$ ) and *EF* is the IPCC emission factor for seasonally rice cultivation ( $\text{g CH}_4 \text{ m}^{-2} \text{ year}^{-1}$ ) (IPCC, 1997).

---

Accurate rice paddy annual harvested area is necessary to obtain an accurate estimate of CH<sub>4</sub> emissions from rice cultivation. The IPCC emissions factor for seasonal rice cultivation was determined based on an arithmetic mean of direct measurements of the season CH<sub>4</sub> emissions from 10 different countries from Asia, Australia, Europe and USA (IPCC, 1997).

A unique aspect of rice cultivation is the presence of irrigation/flooding during the transplanting phase. During the growth stages (vegetative, generative and ripening phases) up to harvesting, the canopy of a rice paddy changes for 4–5 months for one season of rice cultivation depending on the variety of rice being grown. Thus, these two special characteristics can be used as signatures for differentiating rice fields with other land covers (Rudiyanto et al., 2019; Zhang et al., 2020). To detect the presence of water during transplanting, Normalized Difference Snow Index (NDSI) time series spectra were used while canopy changes were detected using Normalized Difference Vegetation Index (NDVI) time series spectra. During the transplanting or flooding phase, a peak in NDSI time series spectra appears. (NDSI is not only useful to identify snow, but also the presence of water/flooding. see below for how indices were derived) Thus, the phenology based algorithm is very useful for mapping rice area and cropping intensities (Dong and Xiao, 2016).

The global annual map of harvested rice at 500 m was determined using time series MODIS data and a phenology-based algorithm implemented in the Google Earth Engine platform. The 8-day composite surface reflectance products from two EOS-MODIS: MOD09A1.006 Terra Surface Reflectance (MODIS/006/MYD09A1) and MYD09A1.006 Aqua Surface Reflectance at 500 m spatial resolutions were used to generate monthly composites two spectral indices namely NDVI (Eq.2) and NDSI (Eq. 3) as follows:

$$NDVI = (NIR - RED)/(NIR + RED) \text{ (Eq. 2)}$$

$$NDSI = (GREEN - SWIR)/(GREEN + SWIR) \text{ (Eq. 3)}$$

The EOS-MODIS (MOD12Q1) provides cropland identification based on the land cover scheme of the International Geosphere-Biosphere Programme (IGBP) and was used to mask non-croplands in the region of interest to create a rice cultivation map. Table 1 shows lists of datasets that are used for estimating harvested rice cultivation extent.

Global spatial temporal CH<sub>4</sub> emissions from rice cultivation were obtained by applying CH<sub>4</sub> emission factors to the satellite-derived rice cultivation map. The output of products was annual global CH<sub>4</sub> emissions from rice cultivation with a 500 m spatial resolution. Zonal statistics was used to calculate annual CH<sub>4</sub> emissions from rice cultivation by country and/or province administrative levels. In summary, workflow for estimating CH<sub>4</sub> emissions from rice cultivation using satellite-based annual rice cultivation map is presented in Figure 1.

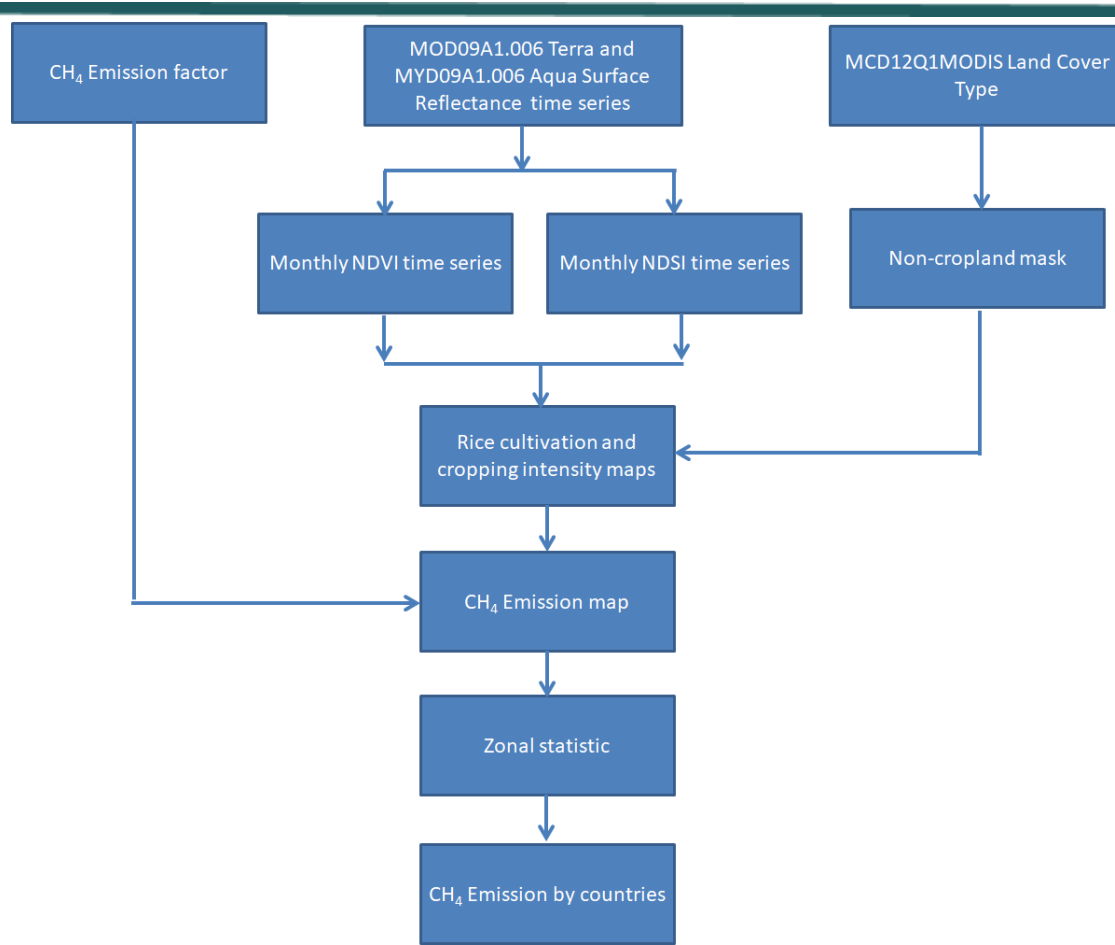


**Figure 1.** Workflow for estimating CH<sub>4</sub> emissions from rice cultivation using satellite-based annual rice cultivation map.

## 2.1 Remote Sensing

**Table 1.** Sources of datasets that are used for estimating harvested rice cultivation extent.

| Satellite/Sensor:   | Bands Employed:  | Used to:   | Temporal and Spatial Resolution, and coverage: |
|---|--|--|--|
| <ul style="list-style-type: none"> <li>- MOD09A1.006 Terra Surface Reflectance (MODIS/006/MYD09A1)</li> <li>- MYD09A1.006 Aqua Surface Reflectance (MODIS/006/MOD09A1)</li> </ul> | sur_refl_b01 (red)<br>sur_refl_b02 (NIR)<br>sur_refl_b04 (green)<br>sur_refl_b05 (SWIR1) for generating 2 indices: NDVI and NDSI | Identify rice cultivation and cropping intensities | 8-day, 500 m, global                           |
| MODIS Land Cover Type (MODIS/006/MCD12Q1)   | LC_Type1 (the land cover scheme of International Geosphere-Biosphere Programme, IGBP)  | Mask non-cropland                                  | Annual, 500 m, global                          |

### 3. Results and Discussion

#### 3.1 Selected inventories

The Climate TRACE rice cultivation sector estimates emissions from rice fields. To compare similar emission sources, the following inventory and category is selected:

- Food and Agriculture Organization, FAOSTAT: Category 'Rice Cultivation' defined as Greenhouse gas (GHG) emissions from rice cultivation that consist of methane gas from the anaerobic decomposition of organic matter in paddy fields. The FAOSTAT emissions database is computed following Tier 1 IPCC 2006 Guidelines for National GHG Inventories.

#### 3.2 Results

In this study we estimate harvested rice cultivation area from MODIS data for the year 2020. An emission factor is applied, set to 20 g/m<sup>2</sup>/season, which is the average value of CH<sub>4</sub> flux from the field measurements (IPCC, 2017). The results of 500 m spatial distribution of annual CH<sub>4</sub> emission estimates from rice cultivation in 23 major producing rice countries are shown in Figure 2.

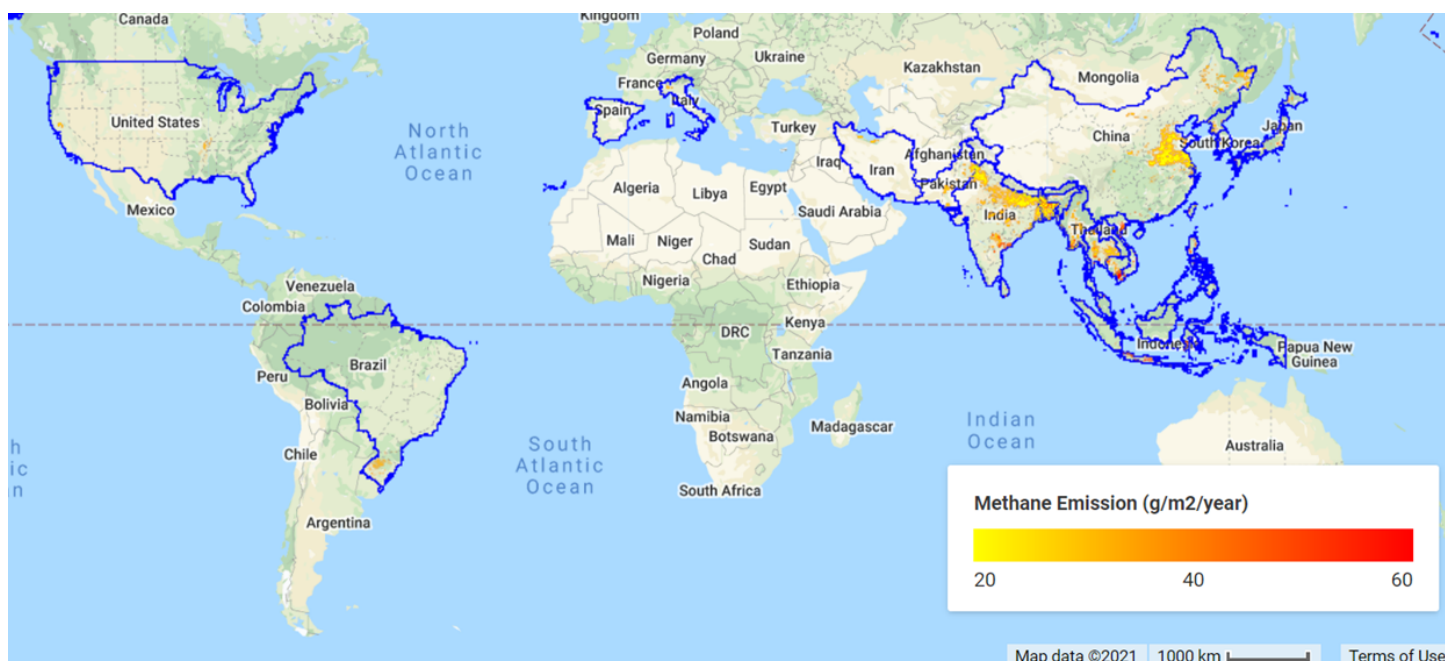


**Figure 2.** Spatial distribution of estimate of annual CH<sub>4</sub> emission for the year 2020 from rice cultivation in 23 major producing rice countries (outlined in blue) derived from Paddy Watch using satellite-based data.

Figure 3a shows the correlation between global CH<sub>4</sub> emission from Paddy Watch-2020 and FAOSTAT-2019 and Figure 3b shows the correlation between harvested rice cultivation from Paddy Watch-2020 and FAOSTAT-2019. No FAOSTAT-2020 is available for comparison due to time lag with compiling information. There is a strong linear relationship between Paddywatch and FAO country statistics. Most data fall in the 95% confidence interval of the linear regression line.

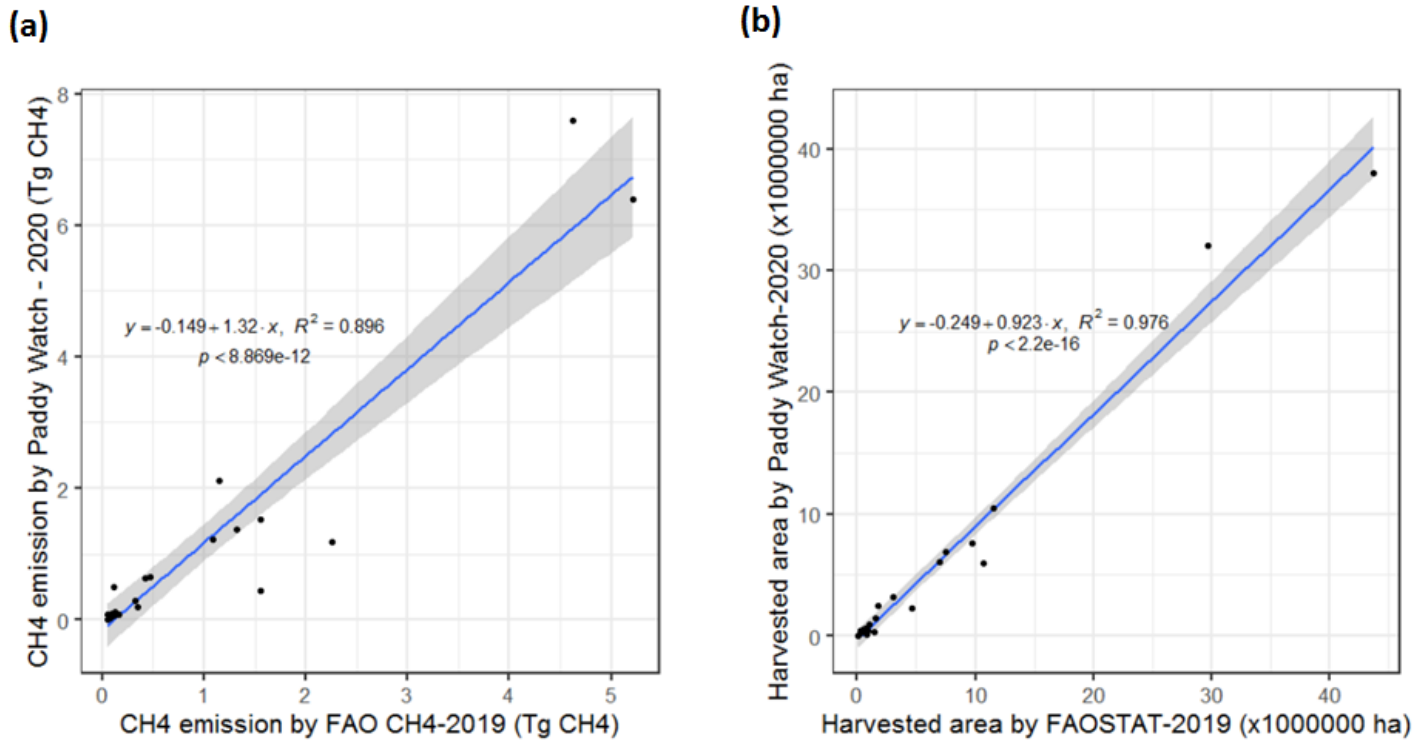


**Figure 3.** Scatter plots between (a) between global CH<sub>4</sub> emission and (b) harvested rice cultivation from Paddy Watch-2020 and FAOSTAT-2019 with 95% confidence interval displayed (grey shaded area).

Table 2 shows the annual CH<sub>4</sub> emission from rice cultivation and the harvested rice cultivation area from FAOSTAT-2019 as well as the absolute relative difference with our estimates. The absolute relative difference values (ratio between the absolute difference of the estimate from this study and FAO-CH<sub>4</sub> with the estimate) range between 0-341% for the annual CH<sub>4</sub> emission from rice cultivation; and 3-139% for harvested rice cultivation area. In total, the harvested rice cultivation from Paddy Watch-2020 is about 12% lower than FAOSTAT data; while the CH<sub>4</sub> emission is around 16% larger. The larger value is due to the larger emission factor used by Paddy Watch.

**Table 2.** Estimate of annual CH<sub>4</sub> emission from rice cultivation and harvested rice cultivation for 23 major rice-producing countries. *Note- On the Climate TRACE website, we report each country's rice emission as tCO<sub>2</sub>eq by multiplying tCH<sub>4</sub> by using Global Warming Potential values for 100 year time horizon AR5 (GHG Protocol, 2021).*

| Country                  | Methane emission (Tg CH <sub>4</sub> ) |                            | Absolute relative difference of CH <sub>4</sub> emission (%) | Harvested rice area (ha) |                            | Absolute relative difference of harvested rice area (%) |
|--------------------------|--|----------------------------|--|--------------------------|----------------------------|---|
|                          | This study (2020)                      | FAO-CH <sub>4</sub> (2019) |  | This study (2020)        | FAO-CH <sub>4</sub> (2019) |   |
| India                    | 7.600                                  | 4.621                      | 64   | 37,998,818               | 43,780,000                 | 13  |
| China                    | 6.403                                  | 5.214                      | 23   | 32,012,557               | 29,690,000                 | 8   |
| Bangladesh               | 2.107                                  | 1.145                      | 84   | 10,533,907               | 11,516,553                 | 9   |
| Indonesia                | 1.188                                  | 2.258                      | 47   | 5,940,978                | 10,677,887                 | 44  |
| Thailand                 | 1.521                                  | 1.554                      | 2  | 7,603,941                | 9,715,358                  | 22  |
| Viet Nam                 | 1.374                                  | 1.318                      | 4  | 6,872,247                | 7,469,890                  | 8   |
| Myanmar                  | 1.222                                  | 1.083                      | 13   | 6,109,520                | 6,920,875                  | 12  |
| Philippines              | 0.446                                  | 1.556                      | 71   | 2,231,418                | 4,651,490                  | 52  |
| Pakistan                 | 0.640                                  | 0.425                      | 51   | 3,200,601                | 3,033,965                  | 5   |
| Cambodia                 | 0.641                                  | 0.468                      | 37   | 3,206,400                | 3,001,313                  | 7   |
| Brazil                   | 0.490                                  | 0.111                      | 341  | 2,451,437                | 1,710,049                  | 43  |
| Japan                    | 0.284                                  | 0.321                      | 12   | 1,417,582                | 1,542,000                  | 8   |
| Nepal                    | 0.072                                  | 0.156                      | 54   | 358,420                  | 1,491,744                  | 76  |
| United States of America | 0.194                                  | 0.350                      | 45   | 970,727                  | 1,000,390                  | 3   |
| Sri Lanka                | 0.092                                  | 0.102                      | 9  | 462,413                  | 957,596                    | 52  |

|   |               |               |           |                    |                    |           |
|---|---------------|---------------|-----------|--------------------|--------------------|-----------|
| Lao People's Democratic Republic            | 0.021         | 0.077         | 72        | 106,813            | 783,766            | 86        |
| Korea (the Republic of)                     | 0.127         | 0.153         | 17        | 633,513            | 729,814            | 13        |
| Malaysia                                    | 0.113         | 0.122         | 8         | 563,571            | 684,416            | 18        |
| Korea (the Democratic People's Republic of) | 0.085         | 0.083         | 2         | 423,455            | 465,839            | 9         |
| Iran (Islamic Republic of)                  | 0.096         | 0.096         | 0         | 480,013            | 437,231            | 10        |
| Taiwan                                      | 0.083         | 0.049         | 70        | 416,666            | 270,066            | 54        |
| Italy                                       | 0.051         | 0.111         | 54        | 255,077            | 220,030            | 16        |
| Spain                                       | 0.007         | 0.052         | 87        | 33,268             | 103,370            | 68        |
| <b>Total</b>                                | <b>24.857</b> | <b>21.427</b> | <b>16</b> | <b>124,283,342</b> | <b>140,853,642</b> | <b>12</b> |

Table 3 summarizes the results of various schemes of inventory methods applied to estimate global CH<sub>4</sub> emissions from rice cultivation (in Terra grams; Tg). It notes that all of the previous studies use harvested rice area from FAOSTAT, while emission factor values vary based on empirical studies and process based modelling. Commonly the emission factor is derived from the IPCC 2006 Guidelines. To account for the scaling factor which represents rice water regime such as irrigated and rainfed rice areas, Zhang et al. (2016) and Carlson et al. (2017) use the MIRCA2000—Global monthly irrigated and rainfed crop areas around the year 2000 (Portmann et al., 2010). For the CH<sub>4</sub> emission estimates based on process-based modeling, Zhang et al. (2016) use the Dynamic Land Ecosystem Model version 2.0 (DLEM v2.0; Tian et al., 2015) for simulating spatiotemporal variation of CH<sub>4</sub> emissions from global rice fields with various scenarios accounting multiple environmental factors in agricultural management practices such as irrigation, nitrogen fertilizer use, and rotation etc. Since our global estimate of CH<sub>4</sub> emission from rice cultivation was for the year 2020, while the previous studies were for 2000 to 2019, the comparison between our estimated CH<sub>4</sub> results with the previous studies show whether there are significant changes on global CH<sub>4</sub> emission from rice cultivation. By comparison, Table 3 shows that our 2020 CH<sub>4</sub> estimation for rice cultivation from 23 major rice-producing countries is 24.8 Tg CH<sub>4</sub>. This value is similar to the previous years and to other inventories. It also suggests that the amount of CH<sub>4</sub> emitted in 2000 and 2020 has not significantly increased.

**Table 3.** Estimates of total annual global methane emission from rice cultivation using various inventory approaches.

| Year      | Harvested rice area data   | Emission factor  | Total global methane emission (Tg CH <sub>4</sub> /year) | Sources  |
|-----------|--|--|--|--|
| 2020      | Paddy Watch based on MODIS data  | IPCC seasonal emission (20 g/m <sup>2</sup> /season)   | 24.88  | This study (23 major producing rice countries)   |
| 2019      | FAOSTAT-2019   | Emission factor based on IPCC seasonal emission including the scaling factors for rice paddy water regime and a correction factor for organic amendments   | 24.08  | FAO-CH <sub>4</sub> ( <a href="http://www.fao.org/faostat/en/#data/GR">http://www.fao.org/faostat/en/#data/GR</a> ; accessed 25 June 2021) |
| 2000      | Census data from FAOSTAT, Monthly irrigated and rainfed rice areas MIRCA2000 | Emission estimates based on process-based modeling   | 20.45 (18.3–38.8)  | Zhang et al. (2016)  |
| 2000–2017 | FAOSTAT  | <ul style="list-style-type: none"> <li>– FAO-CH<sub>4</sub> (database accessed in February 2019, FAO, 2019)</li> <li>– EDGARv4.3.2 was extrapolated to 2017 using the extended FAO-CH<sub>4</sub> emissions</li> <li>– USEPA (2012)</li> </ul> | 30 (25–38)   | Saunio et al. (2020)   |
| 2000      | FAO's AQUASTAT database or FAOSTAT and MIRCA2000                             | IPCC emission and scaling factors  | 28.3   | Carlson et al. (2017)  |



---

### 3.3 Discussion of Results

The inventory approach is commonly used to estimate global CH<sub>4</sub> emissions from rice cultivation. The inventory method estimates CH<sub>4</sub> emissions from rice cultivation based on harvested rice area from country-specific statistical data, emission factor, and scaling and correction factors (IPCC, 1997). Harvested rice areas are usually taken from FAOSTAT. This approach relies on the correct country report and does not have spatial detail.

Most studies used the inventory method derived from FAOSTAT (see Table 3), and our study is the first that applied harvested rice cultivation derived from MODIS data using the Paddy Watch method. The Paddy Watch method based on MODIS data that is implemented in Google Earth Engine platform has many advantages, including harvested rice cultivation data that can be provided rapidly and objectively. However, FAOSTAT data relies on country by country reports, which takes years to complete and can contain errors, such as under and overreporting rice area cultivated. The Paddy Watch approach reduces uncertainty since it identifies where rice was planted, grown and harvested. The high correlation between harvested rice cultivation areas from Paddy Watch-2020 and FAOSTAT-2019 suggests that the accuracy of Paddy Watch is excellent.

The difference between harvested rice cultivation area from statistical data and remote-sensing estimates can be due to two factors: (i) MODIS data which have moderate spatial resolution lead to mixed pixels, where rice fields and non-rice fields are combined. This can overestimate area, especially in lowland regions and have a low ability to detect small rice field patches in upland regions (Frolking et al 1999, Seto et al 2000); and (ii) political and policy factors (Yan et al., 2019) such as determination of the amount of subsidies for fertilizers and evaluation of achievement of government programs in the agricultural sector.

Other factors that contribute to discrepancy in CH<sub>4</sub> emission are from different emission and scale factors that are related to water regime and organic amendment. These values give high uncertainty since the availability of these data are limited and quite variable.

### 4. Conclusions and next steps

Here, we successfully applied the harvested rice cultivation area derived from MODIS data for estimating global CH<sub>4</sub> emission from rice cultivation. We estimated the global CH<sub>4</sub> emission from rice cultivation from 23 major rice producing countries, representing 73% of global rice area for the year 2020 (based on FAOSTAT-2019). From these countries, the estimated global CH<sub>4</sub> emissions from rice was 24.8 Tg CH<sub>4</sub> for 2020.

The application of the Paddy Watch approach for deriving the spatially-resolved global harvested rice cultivation area will help provide updated rice emissions data in a timely fashion. To improve the estimated CH<sub>4</sub> emission from rice cultivation, regional emission factors need to be identified. Additionally, a finer resolution of the global harvested rice cultivation map that generated from Sentinel-1 & 2 data will highly enhance the spatial detail of rice areas. In addition, supporting data related to emission factors and scaling

such as water regime and organic amendment are required in order to improve and reduce uncertainty in rice emission estimates.

## 5. Bibliographical References

1. Carlson, K.M., Gerber, J.S., Mueller, N.D., Herrero, M., MacDonald, G.K., Brauman, K.A., Havlik, P., O'Connell, C.S., Johnson, J.A., Saatchi, S., West, P.C., 2017. Greenhouse gas emissions intensity of global croplands. *Nat. Clim. Chang.* 7, 63–68. <https://doi.org/10.1038/nclimate3158>
2. Dong, J., Xiao, X., 2016. Evolution of regional to global paddy rice mapping methods: A review. *ISPRS J. Photogramm. Remote Sens.* 119, 214–227. <https://doi.org/10.1016/j.isprsjprs.2016.05.010>
3. Fung, I., Prather, M., John, J., Lerner, J., Matthews, E., 1991. Three-dimensional model synthesis of the global methane cycle. *Jgr* 96, 13,13–33,65. <https://doi.org/10.1029/91JD01247>
4. Frohling S, Xiao X M, Zhuang Y H, Salas W and Li C S 1999 Agricultural land-use in China: a comparison of area estimates from ground-based census and satellite-borne remote sensing *Glob Ecol Biogeog.* 8 407–16
5. IPCC, 1997. Revised 1996 IPCC Guidelines for National Greenhouse Gas Inventories. Paris.
6. Li, C., Qiu, J., Frohling, S., Xiao, X., Salas, W., Moore III, B., Boles, S., Huang, Y., Sass, R., 2002. Reduced methane emissions from large-scale changes in water management of China's rice paddies during 1980–2000. *Geophys. Res. Lett.* 29, 33–34. <https://doi.org/10.1029/2002GL015370>
7. Portmann, F. T., S. Siebert, and P. Doll (2010), MIRCA2000—Global monthly irrigated and rainfed crop areas around the year 2000: A new high-resolution data set for agricultural and hydrological modeling, *Global Biogeochem. Cycles*, 24, GB1011, doi:10.1029/2008GB003435.
8. Rudiyanto, Minasny, B., Shah, M.R., Che Soh, N., Arif, C., Indra Setiawan, B., 2019. Automated Near-Real-Time Mapping and Monitoring of Rice Extent, Cropping Patterns, and Growth Stages in Southeast Asia Using Sentinel-1 Time Series on a Google Earth Engine Platform. *Remote Sens.* . <https://doi.org/10.3390/rs11141666>
9. Sauniois, M., Bousquet, P., Poulter, B., Peregon, A., Ciais, P., Canadell, J.G., Dlugokencky, E.J., Etiope, G., Bastviken, D., Houweling, S., Janssens-Maenhout, G., Tubiello, F.N., Castaldi, S., Jackson, R.B., Alexe, M., Arora, V.K., Beerling, D.J., Bergamaschi, P., Blake, D.R., Brailsford, G., Brovkin, V., Bruhwiler, L., Crevoisier, C., Crill, P., Covey, K., Curry, C., Frankenberg, C., Gedney, N., Höglund-Isaksson, L., Ishizawa, M., Ito, A., Joos, F., Kim, H.-S., Kleinen, T., Krummel, P., Lamarque, J.-F., Langenfelds, R., Locatelli, R., Machida, T., Maksyutov, S., McDonald, K.C., Marshall, J., Melton, J.R., Morino, I., Naik, V., O'Doherty, S., Parmentier, F.-J.W., Patra, P.K., Peng, C., Peng, S., Peters, G.P., Pison, I., Prigent, C., Prinn, R., Ramonet, M., Riley, W.J., Saito, M., Santini, M., Schroeder, R., Simpson, I.J., Spahni, R., Steele, P., Takizawa, A., Thornton, B.F., Tian, H., Tohjima, Y., Viovy, N., Voulgarakis, A., van Weele, M., van der Werf, G.R., Weiss, R., Wiedinmyer, C., Wilton, D.J., Wiltshire, A., Worthly, D., Wunch, D., Xu, X., Yoshida, Y., Zhang, B., Zhang, Z., Zhu, Q., 2016. The global methane budget 2000–2012. *Earth Syst. Sci. Data* 8, 697–751. <https://doi.org/10.5194/essd-8-697-2016>
10. Sauniois, M., Stavert, A. R., Poulter, B., Bousquet, P., Canadell, J. G., Jackson, R. B., Raymond, P. A., Dlugokencky, E. J., Houweling, S., Patra, P. K., Ciais, P., Arora, V. K., Bastviken, D., Bergamaschi, P., Blake, D. R.,

- Brailsford, G., Bruhwiler, L., Carlson, K. M., Carrol, M., Castaldi, S., Chandra, N., Crevoisier, C., Crill, P. M., Covey, K., Curry, C. L., Etiope, G., Frankenberg, C., Gedney, N., Hegglin, M. I., Höglund-Isaksson, L., Hugelius, G., Ishizawa, M., Ito, A., Janssens-Maenhout, G., Jensen, K. M., Joos, F., Kleinen, T., Krummel, P. B., Langenfelds, R. L., Laruelle, G. G., Liu, L., Machida, T., Maksyutov, S., McDonald, K. C., McNorton, J., Miller, P. A., Melton, J. R., Morino, I., Müller, J., Murguía-Flores, F., Naik, V., Niwa, Y., Noce, S., O'Doherty, S., Parker, R. J., Peng, C., Peng, S., Peters, G. P., Prigent, C., Prinn, R., Ramonet, M., Regnier, P., Riley, W. J., Rosentreter, J. A., Segers, A., Simpson, I. J., Shi, H., Smith, S. J., Steele, L. P., Thornton, B. F., Tian, H., Tohjima, Y., Tubiello, F. N., Tsuruta, A., Viovy, N., Voulgarakis, A., Weber, T. S., van Weele, M., van der Werf, G. R., Weiss, R. F., Worthy, D., Wunch, D., Yin, Y., Yoshida, Y., Zhang, W., Zhang, Z., Zhao, Y., Zheng, B., Zhu, Q., Zhu, Q., and Zhuang, Q. 2020. The Global Methane Budget 2000–2017, *Earth Syst. Sci. Data*, 12, 1561–1623, <https://doi.org/10.5194/essd-12-1561-2020>
11. Seto K C, Kaufmann R K and Woodcock C E 2000 Landsat reveals China's farmland reserves, but they're vanishing fast *Nature* 406 121–21
  12. Tian, H. Q., Q. C. Yang, R. G. Najjar, W. Ren, M. A. M. Friedrichs, C. S. Hopkinson, and S. F. Pan (2015a), Anthropogenic and climatic influences on carbon fluxes from eastern North America to the Atlantic Ocean: A process-based modeling study, *J. Geophys. Res. Biogeosci.*, 120, 757– 772, doi:10.1002/2014JG002760.
  13. Yan, X., Akiyama, H., Yagi, K., Akimoto, H., 2009. Global estimations of the inventory and mitigation potential of methane emissions from rice cultivation conducted using the 2006 Intergovernmental Panel on Climate Change Guidelines. *Global Biogeochem. Cycles* 23, GB2002. <https://doi.org/10.1029/2008GB003299>
  14. GHG Protocol, 2021. Global Warming Potential Values. [https://www.ghgprotocol.org/sites/default/files/ghgp/Global-Warming-Potential-Values%20%28Feb%2016%202016%29\\_1.pdf](https://www.ghgprotocol.org/sites/default/files/ghgp/Global-Warming-Potential-Values%20%28Feb%2016%202016%29_1.pdf)
  15. Zhang, B., Tian, H., Ren, W., Tao, B., Lu, C., Yang, J., Banger, K., Pan, S., 2016. Methane emissions from global rice fields: Magnitude, spatiotemporal patterns, and environmental controls. *Global Biogeochem. Cycles* 30, 1246–1263. <https://doi.org/10.1002/2016GB005381>
  16. Zhang, G., Xiao, X., Dong, J., Xin, F., Zhang, Y., Qin, Y., Doughty, R.B., Moore, B., 2020. Fingerprint of rice paddies in spatial–temporal dynamics of atmospheric methane concentration in monsoon Asia. *Nat. Commun.* 11, 554. <https://doi.org/10.1038/s41467-019-14155-5>

## 6. Public References

<https://www.theland.com.au/story/6891952/paddy-watch/>